Rakenteiden Mekaniikka (Journal of Structural Mechanics)
Vol. 58, No. 1, 2025, pp. 16–32
http://rakenteidenmekaniikka.journal.fi
https://doi.org/10.23998/rm.149371

VERTAISARVIOITU
KOLLEGIALT GRANSKAD
PEER-REVIEWED
www.tsv.fi/tunnus

Thermal convection in a Brinkman porous medium saturated with couple-stress nanofluid: a Galerkin weighted residual approach for different conducting boundaries

Vinod Kumar, Pushap Lata Sharma and Deepak Bains[1]

Summary The thermal instability of a couple-stress nanofluid saturated by a porous media is studied in this article. For the porous medium, the Darcy–Brinkman model is used. The model used for the nanofluid incorporates the effects of Brownian motion and thermophoresis. Three cases of free-free, rigid-rigid and rigid-free boundaries are considered. For this problem, oscillatory convection is ruled out. By using the one-term Galerkin method and normal mode analysis, we solve the eigenvalue problem with Rayleigh number as an eigenvalue. The effects of Darcy number, couple-stress parameter, porosity parameter, modified diffusivity ratio, Lewis number and concentration Rayleigh number are examined analytically and graphically for stationary convection.

Key words: couple-stress nanofluid, thermal instability, porous medium, Brinkman model, Galerkin weighted residue method

Received: 31 October 2024. Accepted: 13 February 2025. Published online: 12 March 2025.

Introduction

A nanofluid is a liquid that contains nanoparticles, usually in the 1–100 nanometre range. These fluids are designed to improve the thermal, electrical and magnetic characteristics of base fluids, such water or oil, by dispersing nanoparticles in them. The author of study [1] was the first to coin this term and covers a noteworthy class of fluids used in heat transmission that is produced by incorporating a very small number of nanoparticles into regular base fluids. Typically, oxide ceramics (Fe_2O_3, ZnO), metal carbides (SiC), metal nitrides (BN, AlN), or metals (Al, Cu) are employed as nanoparticles in nanofluids, while conventional fluids such as water, oil, bio-fluids and polymer solutions serve as base fluids. The study of [2] pointed out that the distinctive attribute of nanofluid is the thermal conductivity escalation. Nuclear reactors, automobile cooling systems, vehicle thermal management systems, heat exchangers, electronic device cooling are among the various uses of nanofluids in technology and engineering. Nanoparticle suspensions are being produced for medical purposes, such as

[1] Corresponding author: deepakbains123@gmail.com

tumour targeting delivery system, brain targeting, MRI contrast enhancement, tissue engineering etc.

Thermal instability is a significant phenomenon with applications in oceanography, atmospheric physics, geophysics and other fields. The author of study [3] examined the effects of seven slips mechanisms and deduced that, Brownian dispersion and heat transfer of suspended nanoparticles are the predominant slide mechanisms in the unavailability of turbulent eddies. Based on these findings, he developed a mathematical illustration of nanofluid. This model was used to study the issues surrounding thermal instability in nanofluids by [4]. The thermal instability in a nanofluid layer saturated in a porous medium was conducted by [5].

The nanoparticles of metal oxides have application in chemical engineering, medicine and electronics, among other industries. Nanofluids are utilized in different scientific and technical domains like textiles, food processing, geophysics, chemical and biological industries. They are further employed to raise the standard of printing technology. Printer ink can be naturally thickened with shear-thinning fluids such sodium alginate, modified starch and cellulose derivatives. [6] analysed the impact of suspended particles on the thermal convection of Jeffrey fluid in a Darcy–Brinkman porous medium. The study highlights how particle interaction affects heat transfer and stability, providing insights into complex fluid behaviour in porous systems. [7, 8] examined convective instability with suspended particles under free-free, rigid-free and rigid-rigid boundary conditions to further clarify stability parameters by employing normal mode and Galerkin 1st approximation approach.

The theory of couple-stress was introduced by [9]. Couple stress fluid applications are important from a theoretical and practical perspective. Synovial fluid acts as a lubricant in a human joint, which is made of articular cartilage and is dynamically loaded. Squeeze film action can preserve the cartilage surface significantly when it forms a fluid film. In the human body, the loaded-bearing synovial joints include the ankle, knee and shoulder joints. These joints have a low coefficient of friction and negligible wear. Positive outcomes for the industrial application of couple stress fluids have been established in several investigations by [10, 11]. When couple stress lubricants are used in place of Newtonian lubricants, journal bearing systems perform better dynamically, have a higher load-carrying capacity, less friction, a lower temperature and enhance fluid film rigidity. Recently, scholars have focused on studying couple stress fluid under various conditions and with varied geometries. [12] investigated how rotation affected a couple-stress fluid in a porous medium that was heated from below. According to analysis of [12], the couple-stress parameter delayed the start of stationary convection in a fluid heated from below in a porous media. The author of study [13] investigated the initiation of convection in a couple-stress fluid in a porous media by means of a thermal non-equilibrium model. In a porous layer saturated with couple-stress fluid, [14] has examined the influences on the beginning of convection caused by various nonuniform fundamental temperature gradients and further, [15, 16] found Coriolis effect and stability of double diffusive convection on couple stress fluid in a porous media. [17] analysed thermal instability in a horizontal layer of couple-stress nanofluid.

Our current investigation is inspired by the works of [4] and [17]. Recognizing the significance of couple-stress nanofluid, as per our knowledge, this type of work has not yet been done; therefore, an attempt has been made to look into the stability of couple-stress nanofluid saturated with porous media using the Brinkman model for three distinct boundary conditions. This study has applications in optimizing heat transfer processes across various fields. It improves energy extraction in geothermal systems, enhances oil recovery, aids in cooling microelectronics and contributes to medical treatments like hyperthermia. Additionally, it helps in environmental remediation, nuclear reactor cooling and the development of advanced materials with tailored thermal properties.

Mathematical model and governing equations

We take into consideration a couple-stress nanofluid that is restricted between two parallel planes at $z^* = 0$ and $z^* = H$ saturating a porous layer with thickness H. We use Cartesian coordinates, where the origin is at the bottom of permeable medium, the horizontal coordinate is x and the vertical coordinate is z which increases upwards. The layer experiences heat from below, which is counteracted by aligned gravitational force g = (0, 0, –g). We consider a porous medium with porosity ε, permeability K and hydrostatic pressure p.

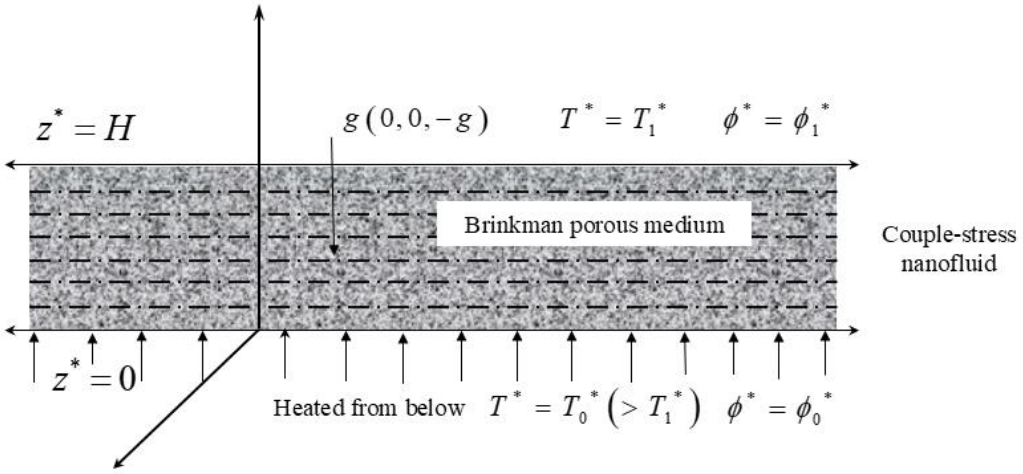

Figure 1: Physical configuration

For formulating this problem, the following assumptions are made:

1. Fluid is considered to be non-Newtonian as well as incompressible.
2. In order to boost the thermal conductivity of couple-stress nanofluid, the nanoparticles are suspended into it.
3. All thermophysical properties (viscosity, thermal conductivity, specific heat, magnetic permeability, electrical conductivity, and electrical resistivity) in case of nanofluid are assumed to be constant in the analytical formulation.
4. In case of nanoparticles, these thermophysical properties are not constant and depend upon volume fraction of the nanoparticles.
5. Darcy–Brinkman model is considered for porous structure.
6. Boussinesq approximation is employed.

Accordingly, the governing equations for the analysis of thermal convection in a Brinkman porous medium saturated with a couple-stress nanofluid (by following [4–8], [12–14] and [17]) are mathematically represented as follows for continuity, momentum, energy and nanoparticle concentration, respectively:

$$\nabla^*.\mathbf{v}_D^* = 0 \tag{1}$$

$$\frac{\rho_f}{\varepsilon}\frac{\partial \mathbf{v}_D^*}{\partial t^*} = -\nabla^* p^* + \tilde{\mu}\nabla^{*2}\mathbf{v}_D^* - \frac{1}{K}\left(\mu - \mu_c\nabla^2\right)\mathbf{v}_D^* + \left[\phi^*\rho_p + \left(1-\phi^*\right)\left\{\rho_f\left(1-\beta\left(T-T_1^*\right)\right)\right\}\right]g \tag{2}$$

$$\left(\rho c\right)_m\frac{\partial T^*}{\partial t^*} + \left(\rho c\right)_f\mathbf{v}_D^*.\nabla^* T^* = k_m\nabla^{*2}T^* + \varepsilon\left(\rho c\right)_p\left[D_B\nabla^*\phi^*.\nabla^* T^* + \frac{D_T}{T_1^*}\nabla^* T.\nabla^* T^*\right] \tag{3}$$

$$\frac{\partial \phi^*}{\partial t^*} + \frac{1}{\varepsilon}\mathbf{v}_D^*.\nabla^*\phi^* = D_B\nabla^{*2}\phi^* + \frac{D_T}{T_1^*}\nabla^{*2}T^* \tag{4}$$

where $\mathbf{v}_D^*, \rho_f, \mu, \beta$ represent the velocity, density, viscosity, volumetric expansion coefficient of the fluid respectively, while ρ_p is the density of the particle and $\partial/\partial t^*$ is the material derivative. We have introduced the effective viscosity $\tilde{\mu}$, the effective heat capacity $(\rho c)_m$, and k_m as the effective thermal conductivity of the porous medium. D_B is the Brownian diffusion coefficient and D_T represents the thermophoretic diffusion coefficient. It is assumed that the temperature T and the volumetric fraction of nanoparticles ϕ at the lower wall are T_0^* and ϕ_0^*, while at the upper wall they are T_1^* and ϕ_1^*, respectively. Therefore, the boundary conditions are the following [4]:

$$w^* = 0, \frac{\partial w^*}{\partial z^*} + \lambda_1 H\frac{\partial^2 w^*}{\partial z^{*2}} = 0,\ T^* = T_0^*,\ \phi^* = \phi_0^*\ \text{ at }\ z^* = 0 \tag{5}$$

$$w^* = 0, \frac{\partial w^*}{\partial z^*} - \lambda_2 H\frac{\partial^2 w^*}{\partial z^{*2}} = 0, T^* = T_1^*, \phi^* = \phi_1^*\ \text{ at }\ z^* = H \tag{6}$$

Non-dimensional variables are introduced in the following manner (see [6–8]):

$$\left.\begin{aligned}(x,y,z) = \frac{(x^*,y^*,z^*)}{H}, t = \frac{t^*\alpha_m}{\sigma H^2}, (u,v,w) = \frac{(u^*,v^*,w^*)H}{\alpha_m},\\ p = \frac{p^*K}{\mu\alpha_m}, \phi = \frac{\phi^*-\phi_0^*}{\phi_1^*-\phi_0^*}, T = \frac{T^*-T_1^*}{T_0^*-T_1^*}\end{aligned}\right\} \tag{7}$$

where $\alpha_m = \frac{k_m}{(\rho c)_f}, \sigma = \frac{(\rho c)_m}{(\rho c)_f}$. In a non-dimensional form, the governing equations and boundary conditions can be expressed (by following [4–8] and [17]) as:

$$\nabla.\mathbf{v} = 0 \tag{8}$$

$$\frac{1}{\sigma V_a}.\frac{\partial \mathbf{v}}{\partial t} = -\nabla p + D_a\nabla^2\mathbf{v} - \left(1 - C\nabla^2\right)\mathbf{v} - R_m\hat{e}_z - R_n\phi\hat{e}_z + R_aT\hat{e}_z \tag{9}$$

$$\frac{\partial T}{\partial t} + \mathbf{v}.\nabla T = \nabla^2 T + \frac{N_B}{L_e}\nabla\phi.\nabla T + \frac{N_A\ N_B}{L_e}\nabla T.\nabla T \tag{10}$$

$$\frac{1}{\sigma}\frac{\partial \phi}{\partial t} + \frac{1}{\varepsilon}\mathbf{v}.\nabla\phi = \frac{1}{L_e}\nabla^2\phi + \frac{N_A}{L_e}\nabla^2 T \tag{11}$$

$$w = 0,\quad \frac{\partial w}{\partial z} + \lambda_1\frac{\partial^2 w}{\partial z^2} = 0,\quad T = 1,\quad \phi = 0\quad \text{at}\quad z = 0 \tag{12}$$

$$w = 0,\quad \frac{\partial w}{\partial z} - \lambda_2\frac{\partial^2 w}{\partial z^2} = 0,\quad T = 0,\quad \phi = 1\quad \text{at}\quad z = 1 \tag{13}$$

where $\Pr = \frac{\mu}{\alpha_m\rho_f}$ is the Prandtl number, $Da = \frac{K}{H^2}$, is the Darcy number, $D_a = \frac{\mu K}{\mu H^2}$ is the Darcy Brinkmann number, $C = \frac{\mu_c}{\mu H^2}$ is the Couple-stress parameter, $L_e = \frac{\alpha_m}{D_B}$, is the Lewis

number, $V_a = \dfrac{\varepsilon \mu H^2}{\alpha_m \rho_f K}$, is the Vadasz number, $R_a = \dfrac{\rho_f g \beta K H \left(T_0^* - T_1^*\right)}{\mu \alpha_m}$, is the thermal Rayleigh–Darcy number, $R_m = \dfrac{\left[\rho_p \phi_1^* + \rho\left(1-\phi_1^*\right)\right] g K H}{\mu \alpha_m}$, is the basic density Rayleigh number, $R_n = \dfrac{\left(\rho_p - \rho\right)\left(\phi_1^* - \phi_0^*\right) g K H}{\mu \alpha_m}$, is the nanoparticle concentration Rayleigh number, $N_A = \dfrac{D_T \left(T_0^* - T_1^*\right)}{D_B T_c^* \left(\phi_1^* - \phi_0^*\right)}$, is the modified diffusivity rate, $N_B = \dfrac{\varepsilon \left(\rho c\right)_p}{\left(\rho c\right)_m}\left(\phi_1^* - \phi_0^*\right)$, is the modified particle-density increment.

Basic solutions

For nanofluids, the time-independent fundamental states are written (by following [6–8]) as:

$$\mathbf{v}\left(u,v,w\right) = \mathbf{0} \Rightarrow u = v = w = 0, T = T_b\left(z\right), \phi = \phi_b\left(z\right), p = p_b\left(z\right) \tag{14}$$

By using equation (14) in equation (8)–(11), these equations reduce to

$$-\frac{dp_z}{dz} - R_m \hat{e}_z - R_n \phi_b \hat{e}_z + R_a T_b \hat{e}_z = 0 \tag{15}$$

$$\frac{d^2 T_b}{dz^2} + \frac{N_B}{L_e}\frac{d\phi}{dz}.\frac{dT_b}{dz} + \frac{N_A N_B}{L_e}\left(\frac{dT_b}{dz}\right)^2 = 0 \tag{16}$$

$$\frac{d^2 \phi_b}{dz^2} + N_A \frac{d^2 T_b}{dz^2} = 0 \tag{17}$$

The solution of equation (17), by using boundary conditions (12) and (13), is of the form

$$\phi_b = -N_A T_b + \left(1 - N_A\right) z + N_A \tag{18}$$

After neglecting the higher order term in equation (16) and substituting the value of ϕ_b from equation in equation (16), we get

$$\frac{d^2 T_b}{dz^2} + \frac{\left(1-N_A\right) N_B}{L_e}.\frac{dT_b}{dz} = 0 \tag{19}$$

The solution of equation (19), by using boundary conditions (12) and (13), is finally

$$T_b = \frac{-e^{-\left(1-N_A\right)N_B/L_e}\left[1 - e^{-\frac{\left(1-N_A\right)N_B}{L_e}\left(1-z\right)}\right]}{1 - e^{-\left(1-N_A\right)N_B/L_e}} \tag{20}$$

According to the study of [3], for most nanofluids investigated so far $\dfrac{L_e}{\left(\phi_1 - \phi_0\right)}$ is large, of order $10^5 - 10^6$, and since the nanoparticle fraction decrement $\left(\phi_1 - \phi_0\right)$ is not smaller than 10^{-3}, this means that L_e is large, of order $10^2 - 10^3$. Typical values of N_A is not smaller than about 10. Then, the exponents in equation (20) are small. By expanding the exponential function into the power series and retaining up to the first-order and negligible other higher-order terms

$\left(i.e.,\ e^{-x} = 1 - x + \frac{x^2}{2!} - \frac{x^3}{3!} + \ldots \approx 1 - x \right)$, one obtains a good approximation for the basic solution $T_b = 1 - z$, and putting this value of T_b in the above equation (18), we get $\phi_b = z$. Thus, the approximated solutions for equation (18) and (20), are obtained as

$$T_b = 1 - z \quad \text{and} \quad \phi_b = z \tag{21}$$

Perturbation solution

For the examination of the stability of the system, a small perturbation to the basic state is introduced (by following [6–8]) as:

$$\mathbf{v}(u,v,w) = 0 + \mathbf{v}'(u,v,w),\ p = p_b + p',\ T = T_b + T',\ \phi = \phi_b + \phi' \tag{22}$$

By applying equation (22) to equations (8)–(13) and linearizing the terms by disregarding the product of perturbed quantities, we obtain the following equations:

$$\nabla . \mathbf{v}' = 0 \tag{23}$$

$$\frac{1}{\sigma V_a}\frac{\partial \mathbf{v}'}{\partial t} = -\nabla p' + D_a \nabla^2 \mathbf{v}' - \left(1 - C\nabla^2\right)\mathbf{v}' + R_a T' \hat{e}_z - R_n \phi' \hat{e}_z \tag{24}$$

$$\frac{\partial T'}{\partial t} - w' = \nabla^2 T' + \frac{N_B}{L_e}\left(\frac{\partial T'}{\partial z} - \frac{\partial \phi'}{\partial z}\right) - \frac{2N_A N_B}{L_e}\frac{\partial T'}{\partial z} \tag{25}$$

$$\frac{1}{\sigma}\frac{\partial \phi'}{\partial t} + \frac{1}{\varepsilon}w' = \frac{1}{L_e}\nabla^2 \phi' + \frac{N_A}{L_e}\nabla^2 T' \tag{26}$$

$$w' = 0,\quad \frac{\partial w'}{\partial z} + \lambda_1 \frac{\partial^2 w'}{\partial z^2} = 0,\quad T' = 0,\quad \phi' = 0 \quad \text{at} \quad z = 0 \tag{27}$$

$$w' = 0,\quad \frac{\partial w'}{\partial z} - \lambda_2 \frac{\partial^2 w'}{\partial z^2} = 0,\quad T' = 0,\quad \phi' = 0 \quad \text{at} \quad z = 1 \tag{28}$$

By operating $\hat{e}_z.curl.curl$ on equation (24), the six unknowns u', v', w', p', T' and ϕ' can be reduced to three, *i.e.* w', T' and ϕ'. Thus, we have

$$\frac{1}{\sigma V_a}\frac{\partial}{\partial t}\nabla^2 w' - D_a \nabla^4 w' + \left(1 - C\nabla^2\right)\nabla^2 w' - R_a \nabla_H^2 T' + R_n \nabla_H^2 \phi' = 0 \tag{29}$$

where $\nabla^2 = \frac{\partial^2}{\partial x^2} + \frac{\partial^2}{\partial y^2} + \frac{\partial^2}{\partial z^2}$ and $\nabla_H^2 = \frac{\partial^2}{\partial x^2} + \frac{\partial^2}{\partial y^2}$ is the two-dimensional Laplace-operator.

The normal mode analysis

We analyse the disturbances by normal modes as follows (see [18]):

$$\left(w', T', \phi'\right) = \left[W(z), \Theta(z), \Phi(z)\right]\exp\left(ik_x x + ik_y y + nt\right) \tag{30}$$

where, n is the growth rate, k_x and k_y are the wave numbers along x- and y-directions, respectively. By substituting equation (30) into equations (24)–(28), we get

$$\left[\left(D_a + C\right)\left(D^2 - a^2\right)^2 - \left(1 + \frac{n}{\sigma V_a}\right)\left(D^2 - a^2\right)\right]W - R_a a^2 \Theta + R_n a^2 \Phi = 0 \tag{31}$$

$$W+\left(D^2+\frac{N_A}{L_e}D-\frac{2N_AN_B}{L_e}-a^2-n\right)\Theta-\frac{N_B}{L_e}D\Phi=0 \tag{32}$$

$$\frac{1}{\varepsilon}W-\frac{N_A}{L_e}\left(D^2-a^2\right)\Theta-\left(\frac{1}{L_e}\left(D^2-a^2\right)-\frac{n}{\sigma}\right)\Phi=0 \tag{33}$$

$$W=0, DW+\lambda_1D^2W=0, \Theta=0, \Phi=0 \quad \text{at} \quad z=0 \tag{34}$$

$$W=0, DW-\lambda_2D^2W=0, \Theta=0, \Phi=0 \quad \text{at} \quad z=1 \tag{35}$$

where $D=\frac{d}{dz}$, and $a^2=k_x{}^2+k_y{}^2$ is the dimensionless wave number. According to the study of [4] and [18], the boundary conditions should be as follows:

1) Free-free boundaries

$$W=D^2W=\Theta=\Phi=0 \ \text{ at } \ z=0,1 \tag{36}$$

2) Rigid-rigid boundaries

$$W=DW=\Theta=\Phi=0 \quad \text{at} \quad z=0,1 \tag{37}$$

3) Rigid-free boundaries

$$W=DW=\Theta=\Phi=0 \quad \text{at} \quad z=0 \tag{38}$$

$$W=D^2W=\Theta=\Phi=0 \quad \text{at} \quad z=1 \tag{39}$$

The assumed solutions for W,Θ and Φ, for these boundary conditions, are taken as follows: for free-free boundaries,

$$W=W_0\sin\pi z, \Theta=\Theta_0\sin\pi z, \Phi=\Phi_0\sin\pi z \tag{40}$$

for rigid-rigid boundaries,

$$W=W_0\left(z^2-2z^3+z^4\right), \Theta=\Theta_0\left(z-z^2\right), \Phi=\Phi_0\left(z-z^2\right) \tag{41}$$

for rigid-free boundaries,

$$W=W_0\left(3z^2-5z^3+2z^4\right), \Theta=\Theta_0\left(z-z^2\right), \Phi=\Phi_0\left(z-z^2\right) \tag{42}$$

These equations (36)–(42) agree well with the studies of [7] and [8].

Linear stability analysis for free-free boundaries

By substituting equation (40) into equations (31)–(33) and by integrating each term individually form $z=0$ to $z=1$, we get

$$\begin{bmatrix} \left(D_a+C\right)J^2+\left(1+\frac{n}{\sigma V_a}\right)J & -R_aa^2 & R_na^2 \\ 1 & -\left(J+n\right) & 0 \\ \frac{1}{\varepsilon} & \frac{N_A}{L_e}J & \left(\frac{J}{L_e}+\frac{n}{\sigma}\right) \end{bmatrix}\begin{bmatrix} W_0 \\ \Theta_0 \\ \Phi_0 \end{bmatrix}=\begin{bmatrix} 0 \\ 0 \\ 0 \end{bmatrix} \tag{43}$$

where $J=\pi^2+a^2$. The eigenvalue to the system of linear equation (43) is given as

$$R_a = \frac{(J+n)}{a^2}\left\{(D_a + C)J^2 + \left(1 + \frac{n}{\sigma V_a}\right)J\right\} - \frac{R_n\left(\frac{N_A J}{L_e} + \frac{J+n}{\varepsilon}\right)}{\left(\frac{J}{L_e} + \frac{n}{\sigma}\right)} \tag{44}$$

Stationary convection for free-free boundaries

For stationary convection $n = 0$ in equation (44), we obtain

$$R_a^{\,S} = \frac{(D_a + C)\left(\pi^2 + a^2\right)^3 + \left(\pi^2 + a^2\right)^2}{a^2} - \left(\frac{L_e}{\varepsilon} + N_A\right)R_n \tag{45}$$

Results and validation for free-free boundaries

Case (i): when $D_a = 0$, $C = 0$; the critical wave number obtained by minimizing thermal Rayleigh–Darcy number R_a with respect to a^2. Thus, the critical wave number must satisfy

$$\left(\frac{\partial R_a}{\partial a^2}\right)_{a=a_c} = 0$$

and equation (45) gives

$$a_c = \pi \tag{46}$$

Therefore, when $a_c = \pi$, then we get $(R_a)_c = 4\pi^2$. This outcome is consistent with the earlier results of [4] as well as the specific cases identified by [7, 8].

Case (ii): when D_a is large compared with unity; the critical wave number obtained by minimizing thermal Rayleigh–Darcy number R_a with respect to a^2. Thus, the critical wave number must satisfy

$$\left(\frac{\partial R_a}{\partial a^2}\right)_{a=a_c} = 0,$$

and equation (45) gives

$$a_c = \frac{\pi}{\sqrt{2}} \tag{47}$$

Therefore, when $a_c = \frac{\pi}{\sqrt{2}}$, then we get $(R_a)_c = 657.5$. The derived solution corresponds to the original work of [4] and coincides with the special cases formulated by [7, 8].

To figure out the impact of modified diffusivity ratio, porosity, Lewis number, couple-stress parameter, Darcy–Brinkman number and nanoparticle Rayleigh number, the signs of the partial derivatives are noted as follows:

$$\frac{\partial R_a^S}{\partial D_a} > 0, \frac{\partial R_a^S}{\partial N_A} > 0, \frac{\partial R_a^S}{\partial L_e} > 0, \frac{\partial R_a^S}{\partial C} > 0\ \frac{\partial R_a^S}{\partial \varepsilon} < 0, \frac{\partial R_a^S}{\partial R_n} < 0,$$

and these inequalities reveal that while the Darcy–Brinkman number, couple-stress parameter, modified diffusivity ratio and Lewis number have stabilising effects, the porosity parameter and the Rayleigh number of nanoparticles have destabilising consequences.

Linear stability analysis for rigid-rigid boundaries

By using (41) in equations (31)–(33) and integrating each term individually within from $z=0$ to $z=1$ and after applying the Galerkin weighted residue approach, we get

$$\begin{bmatrix} \frac{1}{126}\begin{bmatrix}(D_a+C)\left(504++24a^2+a^4\right)\\ +\left(12+a^2\right)\left(1+\frac{n}{\sigma V_a}\right)\end{bmatrix} & -\frac{R_a a^2}{28} & \frac{R_n a^2}{28} \\ \frac{1}{28} & -\frac{\left(10+a^2+n\right)}{6} & 0 \\ \frac{1}{28\varepsilon} & \frac{N_A}{6L_e}\left(10+a^2\right) & \frac{1}{6}\left(\frac{\left(10+a^2\right)}{L_e}+\frac{n}{\sigma}\right) \end{bmatrix}\begin{bmatrix} W_0 \\ \Theta_0 \\ \Phi_0 \end{bmatrix}=\begin{bmatrix} 0 \\ 0 \\ 0 \end{bmatrix}$$

The eigenvalue to the above system of linear equations is given as

$$R_a=\frac{28}{27a^2}\left[\left(D_a+C\right)\left(504+24a^2+a^4\right)+\left(12+a^2\right)\left(1+\frac{n}{\sigma V_a}\right)\right]\left(10+a^2+n\right) - \frac{\left(N_A\left(10+a^2\right)+\frac{L_e\left(10+a^2+n\right)}{\varepsilon}\right)}{\left(10+a^2+\frac{nL_e}{\sigma}\right)}R_n \tag{48}$$

Stationary convection for rigid-rigid boundaries

For stationary convection, $n=0$ in equation (48), we obtain

$$R_a^{\,s}=\frac{28}{27a^2}\left[\left(D_a+C\right)\left(504+24a^2+a^4\right)+\left(12+a^2\right)\right]\left(10+a^2\right)-\left(N_A+\frac{L_e}{\varepsilon}\right)R_n. \tag{49}$$

Results and validation for rigid-rigid boundaries

Case (i): when $D_a=0$; the critical wave number obtained by minimizing thermal Rayleigh–Darcy number R_a with respect to a^2. Thus, the critical wave number must satisfy

$$\left(\frac{\partial R_a}{\partial a^2}\right)_{a=a_c}=0$$

and equation (49) gives

$$a_c=3.31 \tag{50}$$

Therefore, when $a_c=3.31$, then we get $\left(R_a\right)_c=43.92$. This solution matches the analytical results of [4] and agrees with the specific cases established by [7, 8].

Case (ii): when D_a is large compared with unity; the critical wave number obtained by minimizing thermal Rayleigh–Darcy number R_a with respect to a^2. Thus, the critical wave number must satisfy

$$\left(\frac{\partial R_a}{\partial a^2}\right)_{a=a_c} = 0$$

and equation (49) gives

$$a_c = 3.12 \tag{51}$$

Therefore, when $a_c = 3.12$, then we get $\left(R_a\right)_c = 1750$. This result is similar to the study of [4] and also with special cases observed by [7, 8].

Linear stability analysis for rigid-free boundaries

By substituting equation (42) into equations (31)–(33) and integrating each term individually from $z = 0$ to $z = 1$, after applying the Galerkin weighted residue approach, we get

$$\begin{bmatrix} \frac{1}{630}\left[\begin{matrix}\left(D_a + C\right)\left(4536 + +432a^2 + 19a^4\right) + \\ \left(216 + 19a^2\right)\left(1 + \frac{n}{\sigma V_a}\right)\end{matrix}\right] & -\frac{13}{420}R_a a^2 & \frac{13}{420}R_n a^2 \\ \frac{13}{14} & -\left(10 + a^2 + n\right) & 0 \\ \frac{13}{14\varepsilon} & \frac{N_A}{L_e}\left(10 + a^2\right) & \frac{\left(10 + a^2\right)}{L_e} + \frac{n}{\sigma} \end{bmatrix} \begin{bmatrix} W_0 \\ \Theta_0 \\ \Phi_0 \end{bmatrix} = \begin{bmatrix} 0 \\ 0 \\ 0 \end{bmatrix}$$

The eigenvalue to the above system of linear equation is given by

$$R_a = \frac{28}{507a^2}\left[\left(D_a + C\right)\left(4536 + 432a^2 + 19a^4\right) + \left(216 + 19a^2\right)\left(1 + \frac{n}{\sigma V_a}\right)\right]\left(10 + a^2 + n\right) - \frac{\left(N_A\left(10 + a^2\right) + \frac{L_e\left(10 + a^2 + n\right)}{\varepsilon}\right)}{\left(10 + a^2 + \frac{nL_e}{\sigma}\right)} R_n \tag{52}$$

Stationary convection for rigid-free boundaries

For stationary convection, $n = 0$ in equation (52), we obtain

$$R_a = \frac{28}{507a^2}\left[\left(D_a + C\right)\left(4536 + 432a^2 + 19a^4\right) + \left(216 + 19a^2\right)\right]\left(10 + a^2\right) - \left(N_A + \frac{L_e}{\varepsilon}\right)R_n \tag{53}$$

Results and validation for rigid-free boundaries

Case (i): when $D_a = 0, C = 0$; the critical wave number obtained by minimizing thermal Rayleigh–Darcy number R_a with respect to wave number a^2. Thus, the critical wave number must satisfy

$$\left(\frac{\partial R_a}{\partial a^2}\right)_{a=a_c} = 0$$

and equation (53) gives

$$a_c = 3.27 \tag{54}$$

Therefore, when $a_c = 3.27$, then we get $(R_a)_c = 48.01$. The obtained result is mathematically consistent with the original findings of [4] and also with special cases found by [7, 8].

Case (ii): when D_a is large compared with unity; the critical wave number obtained by minimizing thermal Rayleigh–Darcy number R_a with respect to wave number a^2. Thus, the critical wave number must satisfy

$$\left(\frac{\partial R_a}{\partial a^2}\right)_{a=a_c} = 0$$

and equation (53) gives

$$a_c = 2.67 \tag{55}$$

Therefore, when $a_c = 2.67$, then we get $(R_a)_c = 1139$. This result matches both the original findings of [4] and also with the special cases found by [7, 8].

Results and discussion

In this research, we have used the Brinkman model for free-free, rigid-rigid and rigid-free conducting boundaries to assess the stability of a couple-stress nanofluid saturated with porous medium. The influence of various parameters such as: the concentration Rayleigh number, Lewis number, Darcy–Brinkman number, couple-stress parameter, modified diffusivity ratio and porosity parameter, on the onset of stationary convection of couple-stress nanofluid has been examined analytically and graphically for free-free, rigid-rigid and rigid-free boundaries. The analytical behaviour of couple-stress nanofluid has been analysed by making use of Galerkin weighted residue method. Figures 2–7 represent the graphical behaviour of thermal convection on couple-stress nanofluids.

Figure 2 illustrates the graph of R_a with respect to wave number a for various values of $D_a = 0.6, 0.8, 1.0$. By fixing other parameters as $N_A = 5, L_e = 1000, \varepsilon = 0.9, R_n = -1, C = 5$, it can be seen from the Figure 2 that R_a goes on increasing, when we increase the value of D_a. Thus, this increasing behaviour of R_a indicate that D_a has stabilising effect on the onset of stationary convection of couple-stress nanofluid and this stabilising nature of D_a has been analysed for all the different conducting boundaries taken in this present study. Also, we have analysed that D_a has more stabilising effect in rigid-rigid boundaries case. Thus, D_a delays the onset of convection of couple-stress nanofluid.

Figure 3 shows the graph of R_a with respect to wave number a for various values of $C = 5, 10, 15$. By fixing other parameters as $D_a = 0.9, N_A = 5, L_e = 1000, \varepsilon = 0.9, R_n = -1,$

Figure 3 indicates that R_a goes on increasing within the rise in the value C. Thus, C has a stabilising effect on stationary convection for the present study and this stabilising behaviour of couple-stress parameter has been observed less for free-free boundary conditions, whereas it is observed more for the consideration of realistic boundary conditions. Here, the stabilising behaviour of the couple-stress parameter indicates that it delays the onset of convection, allowing the system to remain stable for a longer period.

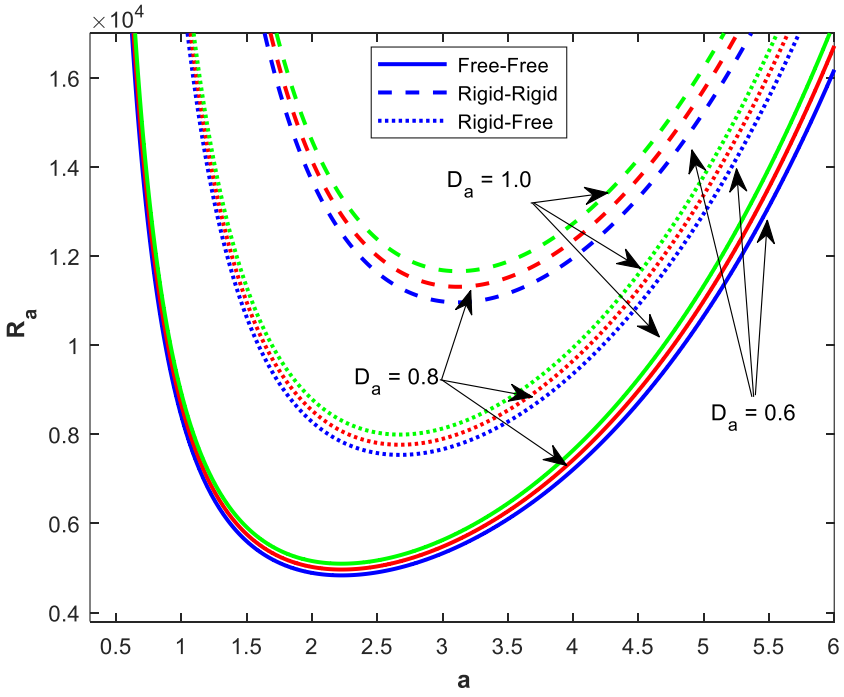

Figure 2: Variation of R_a with wave number a for various values of Darcy–Brinkman number

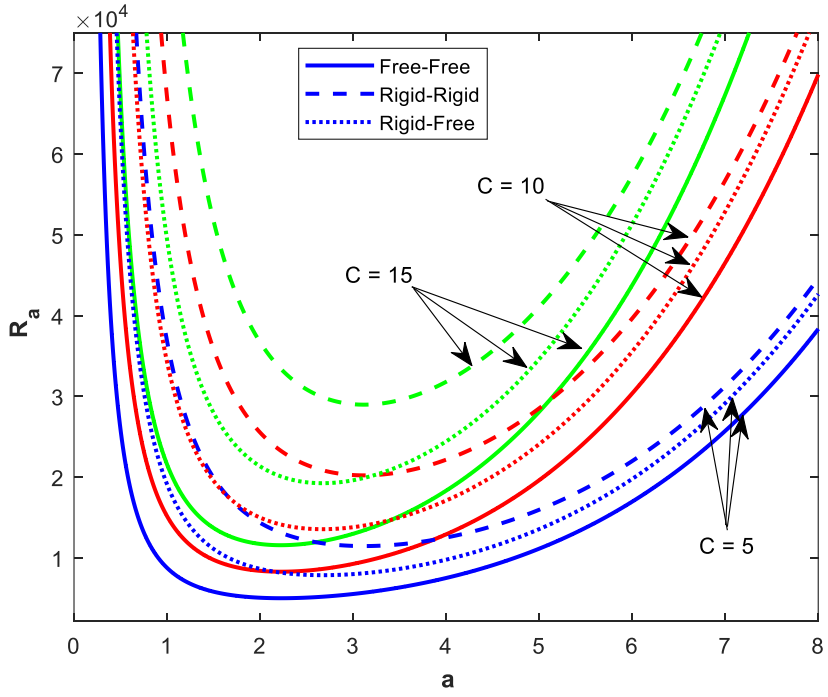

Figure 3: Variation of R_a with wave number a for various values of couple-stress parameter

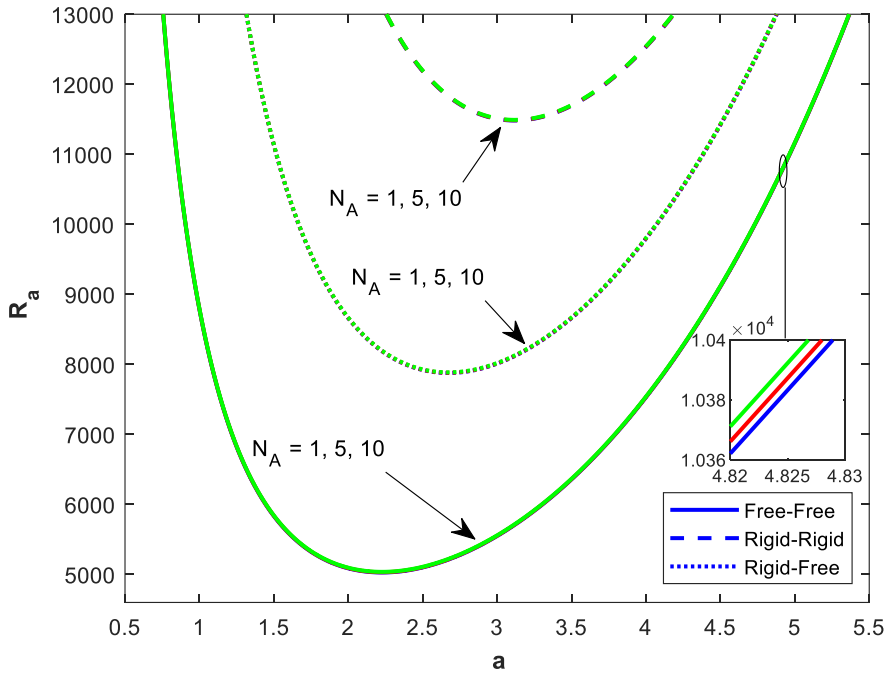

Figure 4: Variation of R_a with wave number a for various values of modified diffusivity ratio

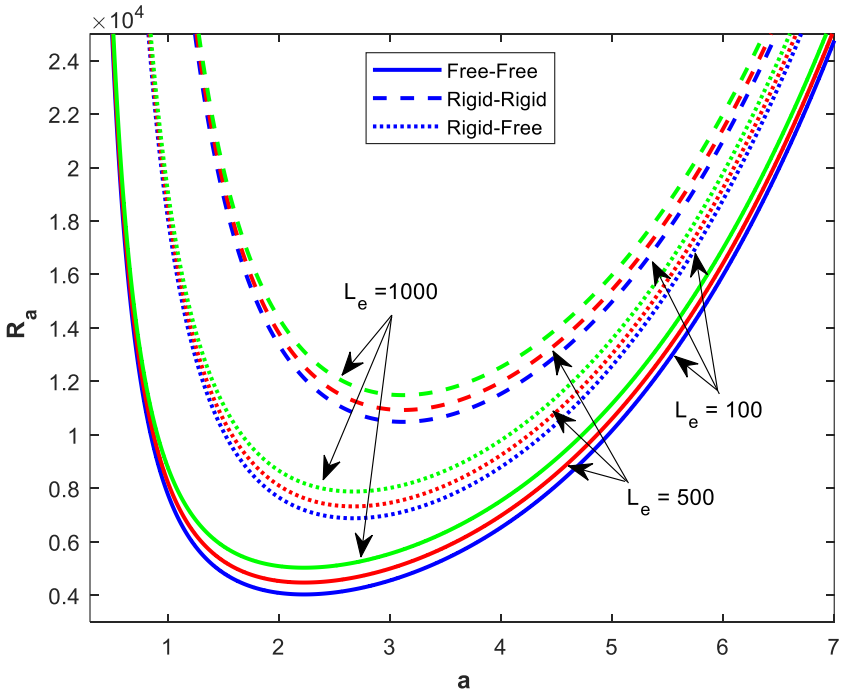

Figure 5: Variation of R_a with wave number a for various values of Lewis number

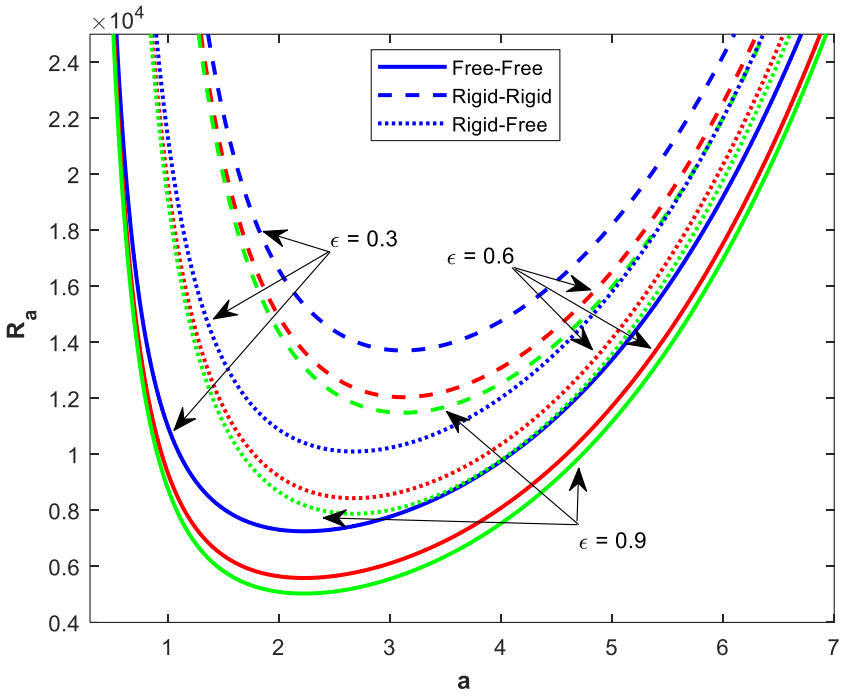

Figure 6: Variation of R_a with wave number a for various values of porosity parameter

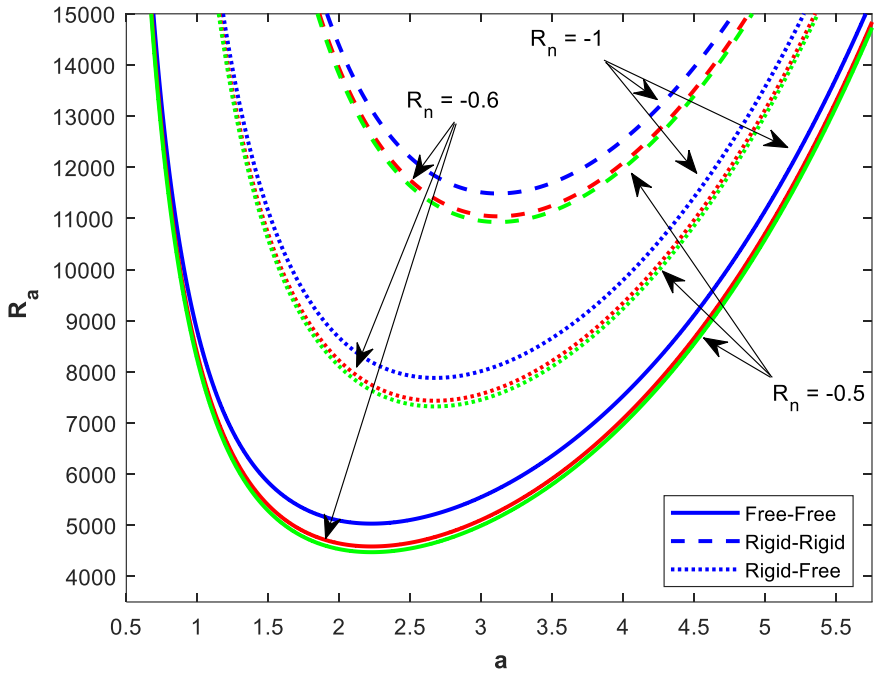

Figure 7: Variation of R_a with wave number a for various values of concentration Rayleigh number

Figure 4 illustrates the graph of R_a with respect to wave number a for various values of $N_A = 1,\ 5,\ 10$. By fixing other parameters as $D_a = 0.9, L_e = 1000, \varepsilon = 0.9, R_n = -1, C = 5$, it is analysed from Figure 4 that as we increase the value of N_A, the density Rayleigh number R_a also goes on increasing. Thus, this behaviour of N_A predicts that it has a stabilising effect on

the onset of convection of couple-stress nanofluid and its more stabilising nature is captured in case of rigid-rigid boundary conditions. Thus, our present investigation confirms that N_A delays the onset of convection of couple-stress nanofluid.

Figure 5 illustrates the graph of R_a with respect to wave number a for various values of $L_e = 100, 500, 1000$. By fixing other parameters as $D_a = 0.9, C = 5, N_A = 5, \varepsilon = 0.9, R_n = -1$, in Figure 5 R_a shows an increasing behaviour, when we increase the value $L_e(100, 500, 1000)$. This increasing behaviour of R_a shows that the Lewis number L_e has a stabilising impact on the stationary convection of couple-stress nanofluid. Our investigation also demonstrates that L_e has a less stabilising effect in free-free boundary condition as compared to rigid-free and rigid-rigid conducting boundaries cases. Thus, L_e delays the onset of convection of couple-stress nanofluid.

Figure 6 illustrates the graph of R_a with respect to wave number a for various values of $\varepsilon = 0.3, 0.6.0.9$. By fixing other parameters as $D_a = 0.9, C = 5\ N_A = 5, L_e = 1000, R_n = -1$, we see that as we increase the value of ε, it imposes the destabilising behaviour on the onset of convection. This can be easily predicted from Figure 6. Our present study demonstrates that ε shows less destabilising effect in case of realistic, i.e., rigid-rigid boundary conditions. Thus, ε accelerates the onset of convection of couple-stress nanofluid.

Figure 7 illustrates the graph of R_a with respect to wave number a for various values of $R_n = -1, -0.6, -0.5$. By fixing other parameters as $D_a = 0.9, C = 5, N_A = 5, L_e = 1000, \varepsilon = 0.9$, Figure 7 shows that R_a goes on decreasing with the increase in the value of R_n. Thus, R_n has destabilising effect on the stationary convection and in this present study its more destabilising nature is found in case of free-free boundary conditions. Thus, R_n enhances the start of convection of couple-stress nanofluid.

Conclusions

In this article, we have analysed thermal instability in a Brinkman porous medium saturated by couple-stress nanofluid for different conducting boundaries. This whole investigation is analysed by making the use of normal mode analysis and Galerkin weighted residue method. The following major conclusions have been drawn from this study:

- Darcy Brinkman number, modified diffusivity ratio, Lewis number and couple-stress parameter have stabilising influence on the system. Due to their stabilising impact on the system, they delay the onset of convection i.e. these parameters allowing the system to remain stable for a longer period. For rigid-rigid conducting boundaries, these parameters describe more stabilising effect as shown in Figure 2–Figure 5.
- Porosity parameter and concentration Rayleigh number enhancing the start of convection on the system due to their destabilising nature for all above mentioned conducting boundaries as shown in Figure 6 and Figure 7. These parameters indicate more destabilising impact for free-free conducting boundaries.
- This study indicates that realistic boundaries (i.e. rigid-rigid conducting boundaries) have greater stabilising impact rather than that of rigid-free and free-free conducting boundaries.

References

[1] S.U. Choi and J.A. Eastman. Enhancing thermal conductivity of fluids with nanoparticles. (No. ANL/MSD/CP-84938; CONF-951135-29). *Argonne National Lab. (ANL), Argonne, IL (United States)*, 1995.

[2] H. Masuda, A. Ebata, K. Teramae and N. Hishinuma. Alteration of thermal conductivity and viscosity of liquid by dispersing ultra-fine particles. *Netsu Bussei*, 7:227–233, 1993. https://doi.org/10.2963/jjtp.7.227

[3] J. Buongiorno. Convective transport in nanofluids. *ASME Journal of Heat and Mass Transfer*, 128:240–250, 2006. https://doi.org/10.1115/1.2150834

[4] A.V. Kuznetsov and D. Nield. Thermal instability in a porous medium layer saturated by a nanofluid: Brinkman model. *Transport in Porous Media*, 81:409–422, 2010. https://doi.org/10.1007/s11242-009-9413-2

[5] D.A. Nield and A.V. Kuznetsov. Thermal instability in a porous layer saturated by a nanofluid. *International Journal of Heat and Mass Transfer*, 52:5796–5801, 2009. https://doi.org/10.1016/j.ijheatmasstransfer.2009.07.023

[6] P.L. Sharma, V. Kumar, D. Bains, P. Lata, A. Kumar and P. Thakur. Effect of suspended particles on the thermal convection in Jeffrey fluid in a Darcy–Brinkman porous medium. *Nova Science Publications*, Inc., USA., 1:113–126, 2024. https://doi.org/10.52305/MHVY6741

[7] P.L. Sharma and D. Bains. Thermal instability in Casson nanofluid with porous medium under the influence of suspended particles: Darcy–Brinkman model. *Special Topics & Reviews in Porous Media: An International Journal*, 16:83–104, 2024. https://doi.org/10.1615/SpecialTopicsRevPorousMedia.2024052335

[8] P.L. Sharma, D. Bains and G.C. Rana. On thermal convection in rotating Casson nanofluid permeated with suspended particles in a Darcy–Brinkman porous medium. *Journal of Porous Media*, 27:73–96, 2024. https://doi.org/10.1615/JPorMedia.2024052821

[9] V.K. Stokes. Couple stresses in fluids. *Theories of Fluids with Microstructure*, 34–80, 1984. https://doi.org/10.1007/978-3-642-82351-0_4

[10] J.R. Lin. Linear stability analysis of rotor-bearing system couple stress fluid model. *Computers & Structures*, 79:801–809, 2001. https://doi.org/10.1016/S0045-7949(00)00189-9

[11] J.R. Lin and Y.M. Lu. Steady-state performance of wide parabolic-shaped slider bearings with a couple stress fluid. *Journal of Marine Science and Technology*, 12:2, 2004. https://doi.org/10.51400/2709-6998.2242

[12] R.C. Sharma. Effect of suspended particles on couple-stress fluid heated from below in the presence of rotation and magnetic field. *Indian Journal of Pure and Applied Mathematics*, 35:973–989, 2004.

[13] M.S. Malashetty, I.S. Shivakumara and S. Kulkarni. The onset of convection in a couple stress fluid saturated porous layer using a thermal non-equilibrium model. *Physics Letter A*, 373:781–790, 2009. https://doi.org/10.1016/j.physleta.2008.12.057

[14] I.S. Shivakumara. Onset of convection in a couple-stress fluid-saturated porous medium: effects of non-uniform temperature gradients. *Archive of Applied Mechanics*, 80:949–957, 2010. https://doi.org/10.1007/s00419-009-0347-5

[15] I.S. Shivakumara, J. Lee, S.S. Kumar and N. Devaraju. Linear and nonlinear stability of double diffusive convection in a couple stress fluid–saturated porous layer. *Archive of Applied Mechanics*, 81:1697–1715, 2011. https://doi.org/10.1007/s00419-011-0512-5

[16] I.S. Shivakumara, S.S. Kumar and N. Devaraju. Coriolis effect on thermal convection in a couple-stress fluid-saturated rotating rigid porous layer. *Archive of Applied Mechanics*, 81:513–530, 2011. https://doi.org/10.1007/s00419-010-0425-8
[17] R. Chand, G.C. Rana and D. Yadav. Thermal instability in a layer of couple stress nanofluid saturated porous medium. *Journal of Theoretical and Applied Mechanics, Sofia*, 47:69, 2017. https://doi.org/10.1515/jtam-2017-0005
[18] S. Chandrasekhar, *Hydrodynamic and Hydromagnetic Stability*, Courier Corporation, New York, USA 2013.

Vinod Kumar
Govt. College Rajgarh
Department of Mathematics, Govt. College Rajgarh, Sirmaur, 173101, India
vinodshimla3@gmail.com

Pushap Lata Sharma, Deepak Bains
Himachal Pradesh University
Department of Mathematics & Statistics, H. P. U., Shimla, 171005, India
pl_maths@yahoo.in, deepakbains123@gmail.com